Science of the Total Environment 509–510 (2015) 104–114

Contents lists available at ScienceDirect

Science of the Total Environment

journal homepage: www.elsevier.com/locate/scitotenv

Pre-industrial and recent (1970–2010) atmospheric deposition of sulfate and mercury in snow on southern Baffin Island, Arctic Canada

Christian Zdanowicz [a,*], Eva Kruemmel [b], David Lean [c], Alexandre Poulain [d], Christophe Kinnard [e], Emmanuel Yumvihoze [d], JiuBin Chen [f], Holger Hintelmann [g]

[a] Department of Earth Sciences, Uppsala University, Villavägen 16, Uppsala 75646, Sweden
[b] Inuit Circumpolar Council of Canada, 75 Albert St., Suite 1001, Ottawa, ON K1P 5V5, Canada
[c] Lean Environmental, P.O. Box 309, Apsley, ON K0L 1A0, Canada
[d] Department of Biology, University of Ottawa, 30 Marie Curie, Ottawa, ON K1N 6N5, Canada
[e] Département des Sciences de l'Environnement, Université du Québec à Trois-Rivières, 3478, Léon-Provancher, Trois-Rivières, QC G9A 5H7, Canada
[f] State Key Laboratory of Environmental Geochemistry, Chinese Academy of Sciences, 46 Guanshi Road, Guiyang 550002, China
[g] Department of Chemistry, Trent University, 1600 West Bank Drive, Peterborough K9J 7B8, Canada

ARTICLE INFO

Article history:
Received 20 November 2013
Received in revised form 16 April 2014
Accepted 22 April 2014
Available online 16 May 2014

Editor: Jim Bennett

Keywords:
Arctic
Mercury
Snow
Ice
Glaciers
Climate change
Air pollution

ABSTRACT

Sulfate (SO_4^{2-}) and mercury (Hg) are airborne pollutants transported to the Arctic where they can affect properties of the atmosphere and the health of marine or terrestrial ecosystems. Detecting trends in Arctic Hg pollution is challenging because of the short period of direct observations, particularly of actual deposition. Here, we present an updated proxy record of atmospheric SO_4^{2-} and a new 40-year record of total Hg (THg) and monomethyl Hg (MeHg) deposition developed from a firn core (P2010) drilled from Penny Ice Cap, Baffin Island, Canada. The updated P2010 record shows stable mean SO_4^{2-} levels over the past 40 years, which is inconsistent with observations of declining atmospheric SO_4^{2-} or snow acidity in the Arctic during the same period. A sharp THg enhancement in the P2010 core ca 1991 is tentatively attributed to the fallout from the eruption of the Icelandic volcano Hekla. Although MeHg accumulation on Penny Ice Cap had remained constant since 1970, THg accumulation increased after the 1980s. This increase is not easily explained by changes in snow accumulation, marine aerosol inputs or air mass trajectories; however, a causal link may exist with the declining sea-ice cover conditions in the Baffin Bay sector. The ratio of THg accumulation between pre-industrial times (reconstructed from archived ice cores) and the modern industrial era is estimated at between 4- and 16-fold, which is consistent with estimates from Arctic lake sediment cores. The new P2010 THg record is the first of its kind developed from the Baffin Island region of the eastern Canadian Arctic and one of very few such records presently available in the Arctic. As such, it may help to bridge the knowledge gap linking direct observation of gaseous Hg in the Arctic atmosphere and actual net deposition and accumulation in various terrestrial media.

1. Introduction

The Arctic is subject to long-range atmospheric contamination by air pollutants from lower-latitude anthropogenic sources (Law and Stohl, 2007). Pollutants such as sulfate aerosols (SO_4^{2-}) impact the radiative balance and water content of the Arctic atmosphere (Quinn et al., 2008), whereas others such as mercury (Hg) can biomagnify and bioaccumulate in marine or terrestrial ecosystems, which increases the risks of toxic exposure in northern populations (Douglas et al., 2012). Although atmospheric SO_4^{2-} and Hg share some common sources (e.g., coal combustion), their emission histories have followed different paths over the last century and reflect an evolving technological and economic context (Hirdman et al., 2010; Smith et al., 2011; Streets et al., 2011). The monitoring of SO_4^{2-} aerosols and gaseous elemental Hg (GEM or Hg^0) in the Arctic atmosphere is presently limited to a few stations, and the longest continuous time series of observations only extends to the early 1980s for SO_4^{2-} (Quinn et al., 2009) and to the mid-1990s for Hg^0 (Cole et al., 2013). This limitation makes identification of long-term trends challenging. Furthermore, changing levels of Hg^0 do not necessarily translate to changing net Hg deposition rates in environmental media because of the high reactivity and volatility of Hg species. However, proxy records of airborne pollution developed from archives such as polar firn and ice cores can serve as useful surrogates for direct measurements of historical Arctic air pollution (e.g., Goto-Azuma and Koerner, 2001) and can determine the atmospheric response to pollution control measures, such as the detection of atmospheric lead (Boutron et al., 1995). Furthermore, net accumulation rates of Hg in the vast glaciated terrestrial areas of the Arctic (~20% of land cover) are presently poorly known. With the

* Corresponding author. Tel.: +46 18 471 3892.
E-mail address: christian.zdanowicz@geo.uu.se (C. Zdanowicz).

http://dx.doi.org/10.1016/j.scitotenv.2014.04.092
0048-9697/

recent adoption of the international Minamata Convention on Mercury (UNEP, 2013), reliable baseline estimates of Hg levels and accumulation rates in various media in the Arctic environment must be established so that the possible impact of future constraining measures on Hg releases may be evaluated.

SO_4^{2-} aerosols have a relatively short atmospheric lifetime of a few weeks (Quinn et al., 2008) and are irreversibly deposited in polar snow by both wet and dry processes (except when snow scouring by wind occurs); however, atmospheric Hg can exist as Hg^0 as well as in its divalent (Hg^{2+}) gas or particulate (Hg_p) phases, and these forms have vastly different atmospheric lifetimes of a few days (Hg^{2+} and Hg_p) to over a year (Hg^0). Furthermore, a large fraction (possibly > 80%) of the Hg deposited in snow may be rapidly re-emitted to the atmosphere because of photochemically-driven changes in the Hg oxidation state (Steffen et al., 2008). The SO_4^{2-} and Hg that accumulate in polar firn, therefore, represent a time-varying fraction of the atmospheric burden of these contaminants. Factors controlling the accumulated SO_4^{2-} fraction in firn include the dry/wet deposition ratio, surface wind strength and snow accumulation rate (e.g., Fischer et al., 1998; Harder et al., 2000). The situation for Hg is more complex because its net deposition rates are linked to ozone and halogen photochemistry in the atmospheric boundary layer (Brooks et al., 2011; Durnford et al., 2012; Toyota et al., 2013).

At present, most historical reconstructions of Hg accumulation in Arctic environments are based on lake sediments or ombotrophic peat, and these archives have their merits and shortcomings (reviewed by Goodsite et al., 2013). Comparatively few archives of Hg accumulation in polar firn and ice exist; however, discontinuous measurements of THg in firn have been reported from central Greenland (e.g., Boutron et al., 1998; Brooks et al., 2011) and a 66-year record of Hg^0 in interstitial firn air was recently developed from the same region (Faïn et al., 2008). Although the latter documents the changing Hg^0 levels in the Arctic air, it does not provide any information on the changing rates of Hg accumulation in the polar firn. Hence, current knowledge of Hg accumulation trends in the vast glaciated regions of the Arctic remains extremely poor.

To address this knowledge gap, a project was initiated as part of the 2007–08 International Polar Year initiative to recover glacial firn and ice cores from multiple sites across the Canadian Arctic Archipelago (CAA) and Greenland, extend earlier glacial records of climatic variables and atmospheric pollution to the present day and define the spatial and recent temporal variability in previously-undocumented trace elements, Hg in particular. One of the sites studied was Penny Ice Cap (~66° N, 6410 km^2), which is the southernmost large ice cap in the CAA and the only one on Baffin Island with an accumulation zone from which ice-core records have been obtained. This region of the CAA is experiencing rapid changes in sea-ice cover (Kinnard et al., 2006; Tivy et al., 2011), which could have an impact on SO_4^{2-} and Hg accumulation in the polar firn.

In previous studies, a Holocene record of atmospheric SO_4^{2-} and nitrate (NO_3^-) deposition on Penny Ice Cap was developed, which extended into the early 1990s (Goto-Azuma and Koerner, 2001; Goto-Azuma et al., 2002). In this article we present an update of the SO_4^{2-} record from Penny Ice Cap, and a new ~40-year record (1970–2010) of total Hg (THg) and monomethyl mercury (MeHg) accumulation from the same site. The study presented here builds on results from an earlier pilot investigation of Hg deposition and release on Penny Ice Cap (Zdanowicz et al., 2013). Findings from the new P2010 core are compared with earlier published results for SO_4^{2-} and THg data measured in earlier historical and prehistorical archived core samples from this site.

2. Materials and methods

2.1. Study site

Penny Ice Cap is located on Cumberland Peninsula (Fig. 1), a mountainous region with deeply incised fjords and glacial valleys. The ice cap

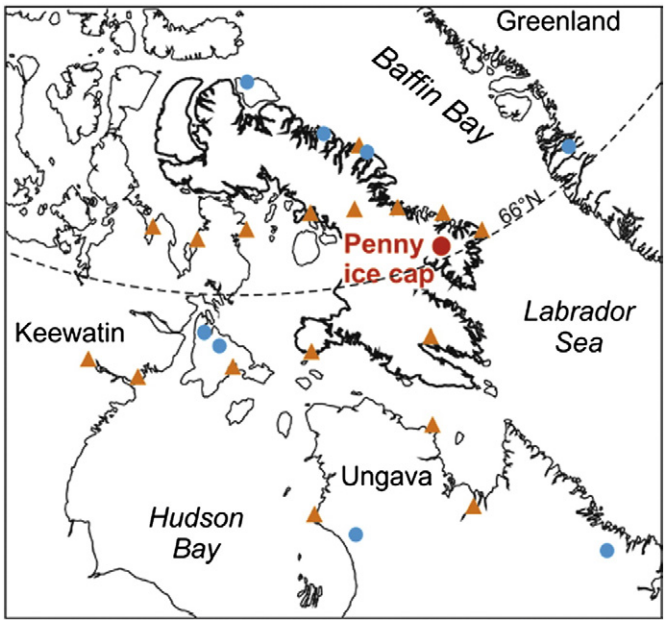

Fig. 1. Location map of the Baffin Island region showing the position of Penny Ice Cap on Cumberland Peninsula. Blue dots indicate sites from which the archives of lake sediment Hg accumulation were developed (Bindler et al., 2001; Cooke et al., 2012; Muir et al., 2009), and orange triangles denote weather stations from which data were obtained for the present study.

summit (~1825 m asl) experiences a mean annual air temperature of −16 °C and accumulation rate of ~0.40 m H_2O a^{-1} (see Section 2.3). Presently, a large part of the winter accumulation at the summit melts in summer and the meltwater percolates into the firn to refreeze as infiltration ice. This process leads to an unquantified vertical redistribution of water-soluble impurities and imposes limits on the temporal resolution of firn and ice core records (Zdanowicz et al., 2012, 2013).

2.2. Firn coring and sampling

A 22.7-m firn core (P2010) was recovered in April 2010 from the summit of Penny Ice Cap using a fiberglass corer (Kovacs Instruments, Lebanon, NH). The coring site was the same site (within GPS error) from which deeper cores were obtained in 1995 (cores P95 and P96: Fisher et al., 1998; Goto-Azuma et al., 2002). Prior to sampling, the corer was cleaned repeatedly in untouched snow and firn. The core was recovered in 0.85-m segments (average) that were measured, weighted, bagged in polyethylene, placed inside opaque coolers and returned frozen to the Geological Survey of Canada (GSC) laboratories in Ottawa where they remained stored in a −25 °C freezer until they were processed. First, the structure, density and electrical conductivity of the core segments were measured (Zdanowicz et al., 2012). The core segments were then sampled inside a metal-free clean cold room at −10 °C by operators wearing non-particulating suits and disposable powder-free gloves. To remove possible external contamination on the core, the following protocol was adapted from previous experiments (Zheng et al., 2006): the outer 2- to 3-mm of each core segment was removed with a stainless steel scalpel, and the shavings from selected cores were collected in sealable, Hg-free Teflon bags (Welch Fluorocarbon, Dover, NH, USA) for analysis. Next, a second 2- to 3-mm thick layer was removed in the same manner, and the shavings were saved in Whirl-Pack bags to be used for major anion (Cl^- and SO_4^{2-}) analyses. These bags have been used and tested routinely for many years and proven to be contamination-free for the determination of major ions at low (ppb) levels. The remaining scraped inner core segments were cut into 10-cm samples (average) with a clean stainless steel saw, placed into Teflon bags and returned to the cold dark storage until

they were melted for Hg and MeHg analyses. To compare the samples from the P2010 core with pre-industrial precipitation, selected archived segments from the earlier P96 core were also prepared for analysis following the protocol described above (for firn) or by a sequential melting procedure (for ice), which is described in Zdanowicz et al. (2012).

2.3. Analysis

Anion analyses (Cl^- and SO_4^{2-}) on the P2010 core samples were performed at the GSC laboratory using a high-performance liquid ion chromatograph (Dionex model 120-DX, Dionex Canada, Oakville, Ontario) and following well-established protocols (Buck et al., 1992). The method detection limits were 5 μg L^{-1} for Cl^- and 20 μg L^{-1} for SO_4^{2-}, and the precision was 30% for Cl^- and 10% for SO_4^{2-}. Glaciochemical data (for ions and Hg) are reported here as mass concentrations in the meltwater and symbolized by brackets, e.g., $[SO_4^{2-}]$. These data are commonly log-normally distributed. Accordingly, we used the geometric means (μ_g) to express averages over a specific depth or time interval unless otherwise specified.

To extend the earlier 1995 ice-core record of major ions (including SO_4^{2-}), the P2010 core data were merged with those from core P95 using the depth–age models described in Section 2.5. The earlier (P95) core had been analyzed at the Nagaoka Institute of Snow and Ice Studies, Japan, using the same protocol as for the P2010 core, which minimized the risk of data incompatibilities arising from different analytical methods. The overlap between the P95 and P2010 cores was estimated to be ~15 years. Fig. 2 shows that for the overlapping sections, the $[SO_4^{2-}]$ distributions in the P2010 and P95 cores are closely comparable and centered at ~115 μg L^{-1}, which indicates that the means of the two sample populations are statistically identical (Mann–Whitney nonparametric *U*-test; $\alpha = 0.05$ and $p = 0.81$). A composite ionic record extending to 2010 was produced by resampling the overlapping data from the P95 and P2010 cores over their common ~15-year period at a uniform one-year time interval and averaging the resulting series together. The correlation coefficient between the two annually-resampled series was 0.51, which translates to an approximate signal-to-noise ratio in the series of ≈1, which is not an uncommon value for such data (Fisher et al., 1985).

THg and MeHg analyses on the new P2010 core were performed at the Laboratory for the Analysis of Natural and Synthetic Environmental Toxins of the University of Ottawa. The core samples were first thawed in a clean room and then split for THg and MeHg analyses. In view of the very low [MeHg] found in polar snow (<0.5 ng L^{-1}), multiple consecutive samples from the P2010 core had to be combined to obtain measurements above detection limits. The resulting sampling resolution for MeHg (~one 0.5-m sample per 2-m depth interval) was therefore coarser than for the major ions and THg (10-cm continuous samples). In total, 212, 221 and 19 samples were analyzed for Cl^- and SO_4^{2-}, THg and MeHg, respectively, excluding blanks and replicates. The THg was determined by cold vapor-atomic fluorescence spectrometry (CV-AFS) as per the US-EPA method 1631E (Environmental Protection Agency, 2002). The "total mercury" was operationally defined by this method as including all of the Hg species oxidized using BrCl and subsequently reduced using $SnCl_2$. Therefore, the measured THg may include Hg^{2+} and Hg^0 as well as Hg_p and organo-complexed Hg compounds. The estimated method detection limit was 0.20 ng L^{-1} (3σ of all blanks), and the precision ±20%. MeHg was determined by capillary gas chromatography coupled with atomic fluorescence spectrometry (GC–AFS) after a preconcentration step (Cai et al., 1996). The detection limit was 0.02 ng L^{-1} (3σ of all blanks), and the estimated precision was ±15%. The archived ice core segments from Penny Ice Cap core P96 were analyzed separately for THg only at the Water Quality Center of Trent University, Ontario, and the analyses also followed the EPA method 1631A (CV-AFS). For these analyses, the method detection limit (3σ of all blanks) was 0.09 ng L^{-1} and the estimated precision was ±7%. Additional details on the methods can be found in Zdanowicz et al. (2013).

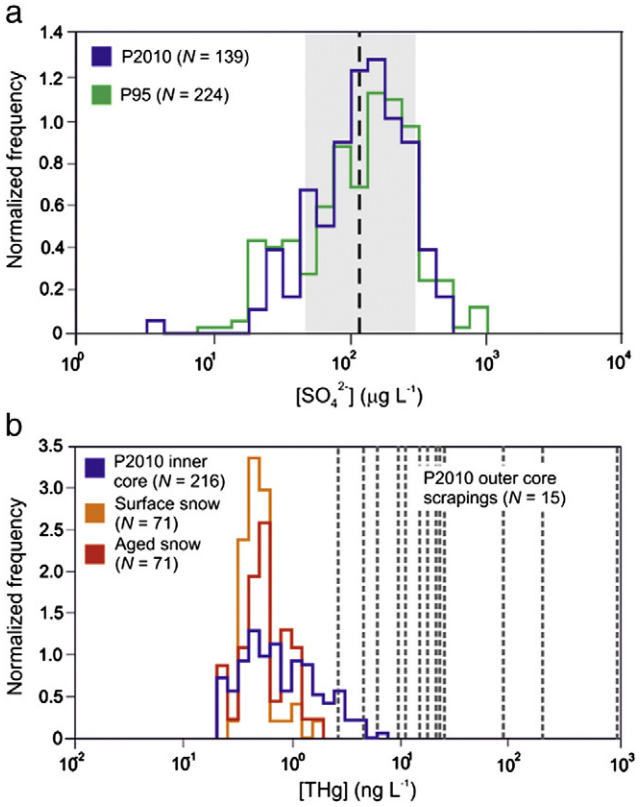

Fig. 2. (a) Normalized frequency histograms of $[SO_4^{2-}]$ in overlapping sections of the P2010 (blue) and P95 (green) firn and ice cores from the summit of Penny Ice Cap. The distributions are centered at an approximate mean of 115 μg L^{-1} (stippled line). (b) Frequency distributions of [THg] measured in inner samples from the P2010 firn core (blue) and near-surface snow samples (orange and red) collected directly in bottles at the ice cap summit (data from Zdanowicz et al., 2013). Dotted lines indicate [THg] values measured in shavings from the outer 2–3 mm of the P2010 firn core.

2.4. Potential Hg losses from sample handling and storage

Zheng et al. (2014) provided evidence of THg losses from untreated snow samples collected in HDPE bottles and exposed to light (up to 30% loss compared with shielded glass bottles) and losses from long-term storage (up to 26% loss over a year). The samples collected for the present study and our pilot study (Zdanowicz et al., 2013) were placed in HDPE bottles (snow) or polyethylene layflat tubing (firn cores) without any preservative because of the logistical difficulty of carrying transportation-restricted chemicals in the field. All of the samples were kept in opaque coolers during transport and cold storage. The time elapsed between the field sample collection and analysis varied from a few weeks to months. Thus, despite all precautions taken, we cannot exclude the possibility of THg losses from our samples. For the firn and ice cores processed in the laboratory, there is a potential for Hg losses by diffusion out of the core segments prior to or during handling. We attempted to mitigate these effects by removing all outer core layers prior to analysis. However, the archived segments of core P96 used in this study were in cold storage for 15 years, and Hg losses were likely to have occurred during such a long period. These would likely be much less important in glacier ice than in shallower porous firn. A possible measure of such losses was obtained by comparing the mean [THg] in the archived segments of core P96 that spanned an interval of ~1960–1992 and in the P2010 core sections that spanned a period of ~1970–1992 (see Section 2.5 for age estimates). All of these core sections are composed of icy firn and have comparable densities. The results produced nearly identical mean [THg] values of 0.50 ng L^{-1} for core P96 and 0.47 ng L^{-1} for core P2010. This suggests that the cores

that have been in cold dark storage for an extended period of time can still yield [THg] comparable to those in recently collected cores of the same site and age, provided that the outer layers are first removed. Although useful, our comparison is presently limited to several core sections, and further evaluation of the long-term storage effects on Hg preservation in snow and ice is warranted. Pending such information, we acknowledge that Hg losses could have occurred in some of our samples, and accordingly, we strived to interpret our findings with the necessary caution.

2.5. Depth–age models

Age models for the P2010 core and relevant sections of the P95 and P96 cores are shown in Fig. 3. The depth–age relationship in the P95 and P96 deep cores follows an ice-flow model approximation (Dansgaard and Johnsen, 1969) that is constrained by parameters such as the total ice thickness and estimated mean ice accumulation rate and by isotopic ($\delta^{18}O$) and volcanic fallout reference horizons, which are described in Fisher et al. (1998) and Goto-Azuma et al. (2002). The estimated dating errors for these age models are provided by Zdanowicz et al. (2012; Table A1). For the main time interval considered in the present study (the last few hundred years), the reference horizons are acidic fallout layers assigned to historical volcanic eruptions, and the most outstanding was that of Laki (Iceland) in 1783, which occurred in most of the deep ice cores drilled in the CAA. Another large and well-defined spike in acidity and SO_4^{2-} was found in two cores drilled in 1995 and attributed to the 1970 eruption of Hekla, also in Iceland (Thorarinsson and Sigvalddason, 1972). We did not find this SO_4^{2-} spike in the new P2010 firn core, which suggests that the borehole did not reach down to the 1970 layer. Alternatively, fallout from this eruption may have been unevenly deposited in snow or removed by wind scouring. This is not unusual because only very large or prolonged eruptions leave unambiguous signatures in ice cores (Zheng et al., 1998). Another signature from a later eruption of Hekla in 1991 (Gudmundsson et al., 1992) was also tentatively identified in the P2010 by a sharp THg spike, which is discussed in Section 3.2. In addition to these volcanic markers, the 1963 peak fallout of β-emitting radioisotopes (^{14}C, ^{137}Cs, ^{3}He, ^{210}Pb, ^{90}Sr, etc.) from pre-moratorium surface nuclear bomb tests was detected using gross β activity measurements on cores drilled in 1979 (Holdsworth, 1984) and 1995 (Grumet et al., 1998). Together, these markers constrain the mean accumulation rate at Penny Ice Cap summit to ~0.40 ± 0.05 m H_2O a^{-1} over the past ~230 years. Based on this value and firn density data, the P2010 core is estimated to represent ~41 ± 5 years of accumulation. The bottom layer of the core may therefore correspond to the mid/late 1960s or early 1970s, but more likely the latter because of the absence of the supposed signal from the Hekla 1970 eruption. Here, we adopt a conservative estimate of 40 years, which is slightly less than what was previously estimated on stratigraphic grounds only (Zdanowicz et al., 2012).

Because of the effects of summer melt and percolation, annual variations in chemical or isotopic profiles cannot be easily resolved in cores from Penny Ice Cap (Goto-Azuma et al., 2002; Grumet et al., 1998). This precludes ascribing specific years in these cores to reference horizons. The tentative identification of the 1991 Hekla signal in the P2010 core suggests dating errors $\leq \pm 5$ years for the past four decades. For deeper and older cores, dating errors can be estimated by Monte-Carlo simulations using realistic (observation-based) estimates of interannual variations in accumulation rates (Zdanowicz et al., 2012). These suggest maximum (conservative) dating errors ranging from ±10 years for the last ~230 years in the P95 core to $\pm 10^3$ years for layers of mid-Holocene age in the shorter P96 core (Fig. 3).

2.6. Meteorological and air mass back-trajectory analyses

To investigate if changes in regional precipitation patterns had an effect on SO_4^{2-} or THg accumulation on Penny Ice Cap, we used archived climatological data from an array of weather stations surrounding southern Baffin Island to compute variations in the total precipitation for the period of 1970–2010 (see Fig. 1 for sites; data from Environment Canada, Mekis and Vincent, 2011; Vincent et al., 2012). We also evaluated the possible effect of changes in atmospheric transport trajectories by computing the 10-day back-trajectories for air masses arriving at the ice cap summit for each day (at 12 PM UTC) from 1970 to 2010 using the Hybrid Single-Particle Lagrangian Integrated Trajectory model (HYSPLIT; version 4.8) of the NOAA Air Resources Laboratory (Draxler and Hess, 1998). Additional details are provided in the Supporting information.

3. Results and discussion

3.1. Down-core profiles of SO_4^{2-} and Hg

Profiles of the physical stratigraphy, density, solid electrical conductivity (ECM) and chemistry ([Cl^-], [SO_4^{2-}], [MeHg] and [THg]) in the

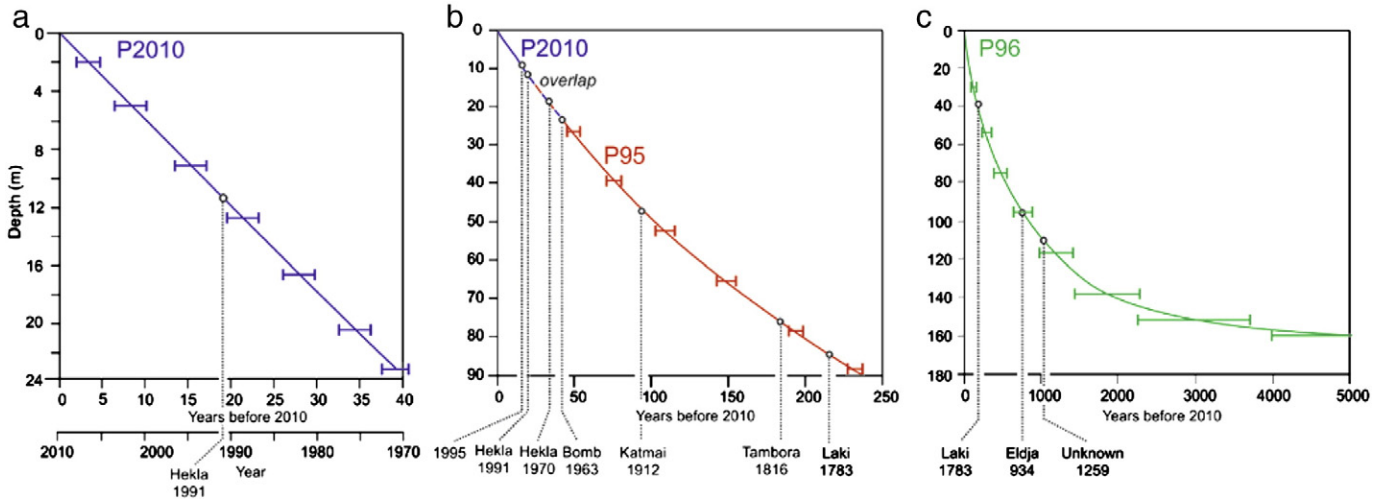

Fig. 3. Depth–age models of the different firn and ice cores used in this study: (a) 1970–2010; (b) last 250 years; and (c) last 5000 years. The depth–age curve for core P2010 in (a) is reproduced in (b) to show the continuity with the earlier P95 core. Ice-core time markers are identified. Estimated errors on predicted ages (95% confidence level) are shown for various depths.

P2010 firn core are presented in Fig. 4, and the descriptive summary statistics for the glaciochemical data are given in Table 1. Detailed results for all of the analyzed samples can be found in the Supporting information for this article. As described in Zdanowicz et al. (2012), the firn stratigraphy at the summit of Penny Ice Cap is characterized by numerous infiltration ice layers and a relatively high mean density (630 kg m^{-3}) because of the effects of meltwater percolation and refreezing in summer. The glaciochemical depth profiles show considerable variability at the centimeter- to meter-scale, but there are no recognizable regular seasonal cycles. A parallel enhancement in the [Cl^-] and [SO_4^{2-}] profiles may reflect post-depositional ion remobilization in the firn by meltwater because these two ions are particularly mobile during elution (Goto-Azuma et al., 1993; Grumet et al., 1998). The [SO_4^{2-}] profile and ECM show a slight increasing trend down-core. This co-variation of [SO_4^{2-}] and conductivity is presumably a result of the predominance of H_2SO_4 aerosols as a source of H^+ (acidity) in Canadian Arctic snow (Koerner and Fisher, 1982). No corresponding down-core trend is found in the [Cl^-] profile. The [THg] profile differs from that of [SO_4^{2-}] in that it shows a slight down-core decrease that is most noticeable in the upper 8 m of the core. A section of core at depths between 10 and 12 m contains layers with markedly higher [THg] of up to 46.20 ng L^{-1}. This is discussed in Section 3.2. Compared to [THg], the [MeHg] profile in the P2010 core shows little variation. Concentrations between 7 and 12 m depths are slightly greater than in higher and lower core sections, but because of the low sampling resolution, it is impossible to ascertain the frequency of such variations.

As previously stated, the anion concentrations in the P2010 core were reasonably consistent with earlier results from the P95 core (Fig. 2a). For THg, we compared results obtained from the firn core with those from the surface (fresh) and subsurface (aged) snow and firn that were previously sampled at the summit of Penny Ice Cap (Fig. 2b; Zdanowicz et al., 2013). These earlier samples ($N = 71$) were collected without a corer directly from the snowpit walls into pre-cleaned Hg-free bottles, and they are considered pristine for THg. The comparison revealed a slight positive skewing towards larger mean [THg] in firn (0.77 ng L^{-1}) and aged snow (0.56 ng L^{-1}) relative to the surface snow (0.50 ng L^{-1}). These findings were consistent with those obtained in our pilot study and suggest that the post-depositional remobilization of THg by meltwater modified its frequency distribution in firn and biased it towards a larger mean than is found in fresh snow (Zdanowicz et al., 2013). Several outer-core shavings of the core P2010 contained [THg] > 10^2 ng L^{-1}, although most had much lower levels. This indicates that some outer core layers were contaminated during or after coring. In contrast, 90% of all of the inner-core samples had [THg] < 3 ng L^{-1}. A single, isolated inner-core sample at a depth of 9.5 m had [THg] = 160 ng L^{-1} and was rejected as an unexplained outlier that was possibly contaminated. Of those inner-core samples that had [THg] ≥ 3 ng L^{-1}, most were found in a section between 10 and 12 m depths (Fig. 4). The highest values in this section (38.26 and 46.20 ng L^{-1}) exceeded the baseline [THg] by a factor greater than 40. The outer-core scrapings from the corresponding core section did not contain exceptionally high [THg] (2.60–4.58 ng L^{-1}), so contamination is unlikely to account for these results. The highest [THg] in this part of the P2010 core occurred immediately below a thick sequence of infiltration ice layers, which raises the possibility that they may be an artifact of meltwater elution and refreezing. However, profiles of [Cl^-] and [SO_4^{2-}] showed no enhancements at a comparably large magnitude at corresponding depths, and evidence of anomalous THg spikes in higher sections of the core with equally thick or thicker infiltration ice layers was not found. At least some of the high [THg] values between 10 and

Table 1
Descriptive statistics for concentrations of Cl^-, SO_4^{2-}, THg and MeHg measured in a 22.7-m core (P2010) from Penny Ice Cap summit, Baffin Island. The values listed under the heading [THg]* were computed without including the anomalously-high (>5 ng L^{-1}) values found between 10 and 12 m, which are presumed to be of volcanic origin (see text).

	[Cl^-]	[SO_4^{2-}]	[THg]	[THg]*	[MeHg]
	μg L^{-1}	μg L^{-1}	ng L^{-1}	ng L^{-1}	ng L^{-1}
N	212	212	221	214	19
Minimum	11.04	3.17	<0.20	0.20	0.06
Maximum	400.47	472.42	46.20	4.68	0.19
Mean μ	82.41	136.51	1.56	0.97	0.11
Standard deviation σ	64.48	88.84	4.29	0.93	0.04
Median	59.93	122.75	0.64	0.63	0.09
Geometric mean μ_g	64.70	109.92	0.72	0.65	0.10
Std. error on μ_g	1.05	1.05	1.08	1.07	1.08

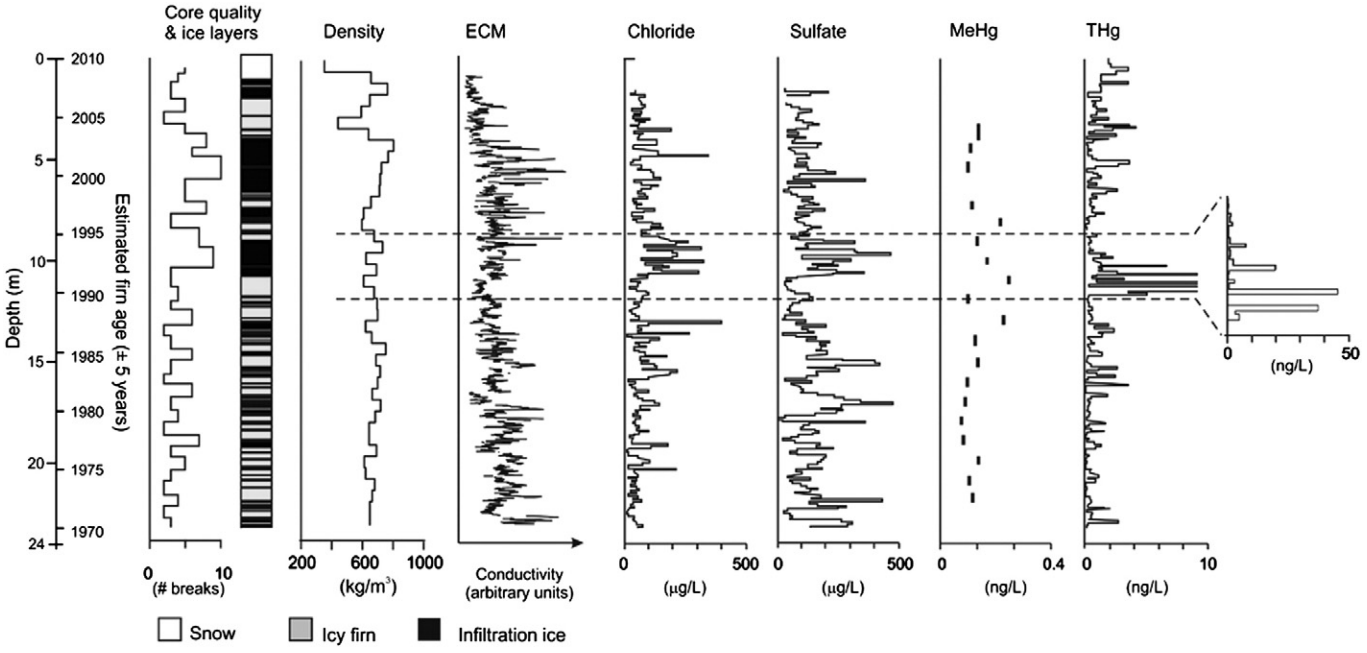

Fig. 4. Physical and chemical properties of the P2010 core. Left to right: core quality and physical stratigraphy (legend below figure); bulk core density (0.55 m increments); solid electrical conductivity; down-core concentrations of Cl^-, sulfate SO_4^{2-}, THg and MeHg. The average sampling interval for Cl^-, SO_4^{2-} and THg was 0.1 m. The horizontal dashed lines bracket the core segment containing the presumed fallout from the Hekla 1991 eruption, in which [THg] > 5 ng L^{-1} was measured (rescaled and enlarged at far right).

12 m were therefore considered to reflect a depositional event, which is described below.

3.2. Temporal variations in SO_4^{2-} and Hg

Time series of non-sea salt sulfate ($nssSO_4^{2-}$), chloride (Cl^-), THg and MeHg in firn and ice cores from Penny Ice Cap are shown in Fig. 5 (period 1780–2010, excluding [MeHg]) and Fig. 6 (last ~50 years, including [MeHg]). The $nssSO_4^{2-}$ and Cl^- data from the P2010 core did not extend beyond 2007 because there was insufficient material in the brittle upper snow and firn layers to provide enough H_2O for both THg and anion analyses.

Using the mean seawater mass ratio of Cl^- to SO_4^{2-}, it was previously estimated that $nssSO_4^{2-}$ accounts for 70 to 95% of the total SO_4^{2-} deposited at Penny Ice Cap in the late 20th century (~1950 to 1995; Fisher et al., 1998; Goto-Azuma et al., 2002). The same calculation performed with data from the P2010 core yielded nss/total SO_4^{2-} mass ratios of 50 to 99% (mean 90%) in the snow and firn since the early 1970s. Much of the $nssSO_4^{2-}$ in the firn may have a marine source, such as biogenic sulfur gas (Li and Barrie, 1993; Rempillo et al., 2011); however, an important but unquantified fraction is thought to be derived from mid-latitude industrial SO_x emissions in North America (Goto-Azuma and Koerner, 2001). Contamination by acidic aerosols from industrial SO_x and/or NO_x emissions first became noticeable in the eastern Arctic ice core and lake sediment layers from the late 19th century (Drevnick et al., 2010; Goto-Azuma and Koerner, 2001; Wolfe et al., 2006). Data from the combined P95 and P2010 cores showed that $nssSO_4^{2-}$ accumulation at Penny Ice Cap increased until the ~mid-1970s or early 1980s, but appears to have remained relatively stable or declined slightly thereafter (Figs. 5a and 6a). During the decade 1960–70, the mean [$nssSO_4^{2-}$] in Penny Ice Cap snow exceeded pre-industrial levels (early 19th century) by a factor of ~4. However, the linear trend in [$nssSO_4^{2-}$] since 1970 (-1 μg L^{-1} a^{-1}) was not significantly different from zero ($\alpha = 0.05$), and the mean [$nssSO_4^{2-}$] in snow accumulated since 2000 (95 μg L^{-1}) was statistically undistinguishable from the mean during the 1960–1970 decade of peak global SO_x emissions (105 μg L^{-1}).

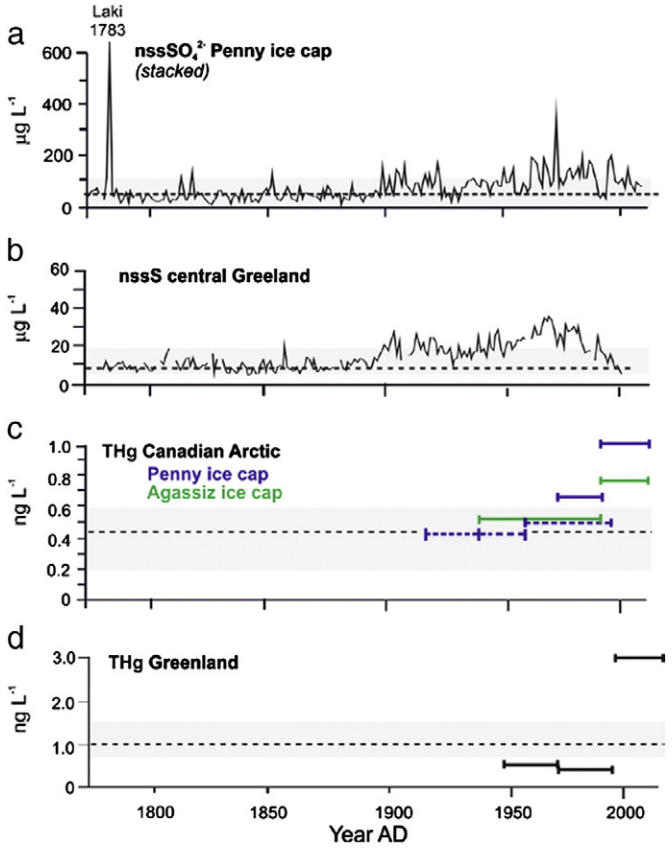

Fig. 5. Historical variations of [$nssSO_4^{2-}$] and [THg] in cores from Penny Ice Cap for the period 1780–2010 compared with other ice-core data. (a) Stacked time series of [$nssSO_4^{2-}$] from cores P95 and P2010. (b) Variations in non-sea salt sulfur (nssS) concentrations in a core from site D4, Greenland (McConnell et al., 2007). (c) [THg] in the cores P96 and P2010 (blue; this study) and Agassiz Ice Cap (green; Zheng et al., 2014). Hatched blue lines are single measurements from archived ice cores (P96) spanning the periods 1920–40, 1940–60 and 1960–90, whereas full blue lines are the geometric means of multiple samples from the P2010 firn core for 1970–1990 and 1990–2010. Green line segments are the corresponding means of multiple samples from Agassiz Ice Cap [THg] data for 1935–1970 and 1990–2009. (d) [THg] in central Greenland firn cores representing the periods 1949–1965, 1965–1989 (Boutron et al., 1998: geometric means) and ~1998–2008 (Brooks et al., 2011: arithmetic mean). Horizontal dashed lines and gray shading on each panel are the estimated geometric mean and range of Holocene pre-industrial [$nssSO_4^{2-}$], [nssS] or [THg] in ice cores from Penny Ice Cap and central Greenland. In (c), the pre-industrial THg data are from archived samples of the P96 core, whereas in (d), the data are from samples of the GISP2 deep core. (Unpublished data supplied by C. Lamborg).

Knowledge of the past Hg accumulation on Penny Ice Cap is limited compared to that of SO_4^{2-}, but some inferences can be made from the available data (Fig. 5c). The range of [THg] measured in the archived core samples (P96) from the Holocene pre-industrial period is <0.20 to 0.59 ng L^{-1} with a mean of 0.41 ng L^{-1} ($N = 15$). These values should be regarded as minimum estimates if any Hg losses occurred during the long-term core storage. The mean [THg] in the P2010 core weighted by the layer density is 0.66 ng L^{-1} ($N = 221$), and three archived core sections from the P96 core spanning the intermediate periods ~1920–40, 1940–60 and 1960–90 produced [THg] equal to 0.43, 0.43 and 0.50 ng L^{-1}, respectively. Translated into accumulation rates (A_{THg}) that assume a constant snowfall rate, data from the P96 archived cores suggest pre-industrial (Holocene) values of A_{THg} in the order of 0.01 to 0.02 μg m^{-2} a^{-1}. For the 20th and 21st centuries, data from the P96 and P2010 cores give estimated values of 0.08 and 0.16 μg m^{-2} a^{-1} (considering dating uncertainties). Together, these estimates provide a ratio of post- to pre-industrial THg accumulation (R_{THg}) between ~4 and 16, which is consistent with estimates derived from lake sediment cores in the Canadian Arctic and western Greenland ($2 \le R_{THg} \le 25$; Bindler et al., 2001; Muir et al., 2009; Cooke et al., 2012; see Fig. 1 for lake core locations). The values of R_{THg} for central Greenland are comparatively uncertain because of the scarcity of available long-term glacial archives of [THg] from this region (Fig. 5d).

An outstanding feature of the P2010 record for the period 1970–2010 is a set of sharp [THg] spikes found at depths (10–12 m) corresponding to the early to mid-1990s (Fig. 6d–e). A similar feature can be seen in a firn sequence analyzed by Zheng et al. (2014) on Agassiz Ice Cap, northern Ellesmere Island (Fig. 6f). Because of possible dating discrepancies between these records, it is uncertain if these features

These findings are inconsistent with ice-core data from central Greenland, which show a marked decline in nssS and acidity (McConnell and Edwards, 2008; Pasteris et al., 2012) after the 1970s (Figs. 5b and 6b), in step with decreasing SO_2 emissions in the Northern Hemisphere and SO_4^{2-} burdens in the Arctic atmosphere (Gong et al., 2010; Quinn et al., 2009; Smith et al., 2011). The lack of evidence for such a decline in the P2010 core is therefore intriguing. A possible explanation is that the trend is obscured by a larger depositional or post-depositional variability of SO_4^{2-} in firn on Penny Ice Cap, compared to locations such as Greenland. A decline in [SO_4^{2-}] could also be masked by a concurrent decline in snow accumulation, but this is unsupported by the available ice-core or meteorological evidence (Zdanowicz et al., 2012, see also Section 3.3). Alternatively, a decline in anthropogenic $nssSO_4^{2-}$ deposition on Penny Ice Cap over recent decades may have been compensated by a larger influx from marine sources linked to the pronounced sea-ice cover reduction over the nearby sectors of Baffin Bay and Hudson Strait, which is where most of the marine aerosols deposited on the ice cap are thought to originate (Grumet et al., 2001; Tivy et al., 2011).

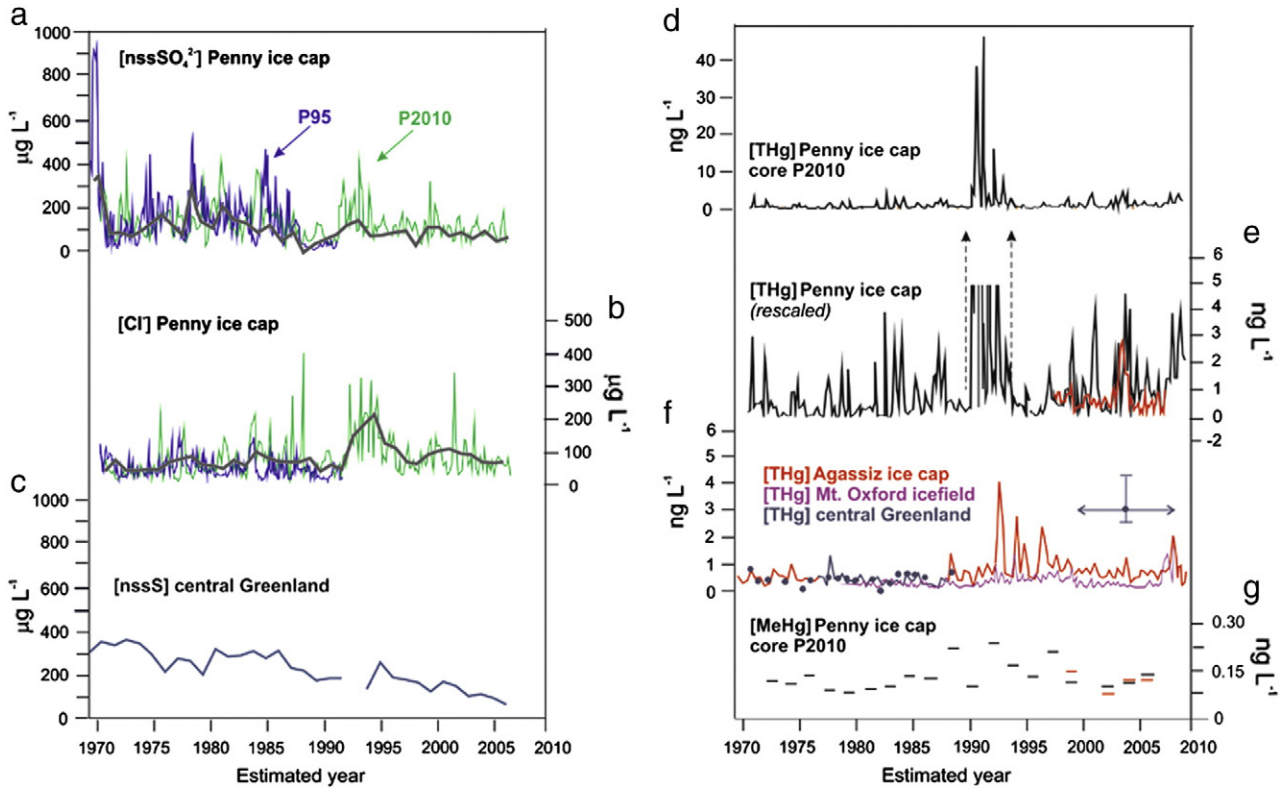

Fig. 6. (a) (b) Overlain records of [nssSO_4^{2-}] and [Cl^-] in cores P95 (blue) and P2010 (green) for the period 1970-2010. Bold lines show trends in the stacked (averaged) time series resampled at a uniform one-year resolution. (c) Annually-resolved record of nssS in the D4 core from central Greenland, which is shown for comparison (McConnell et al., 2007). (d) Records of [THg] in the P2010 core. The time series are re-scaled in (e) to highlight the low-amplitude baseline variations. The red line segment includes measurements from shallow cores taken in 2007 (Zdanowicz et al., 2013) and plotted at the approximate corresponding depths on the P2010 profile. (f) Historical profiles of [THg] in firn from northern Ellesmere Island (Zheng et al., 2014) and central Greenland (Boutron et al., 1998; Brooks et al., 2011). The data point from Brooks et al. is the arithmetic mean of [THg] for the period ~1998–2008. Vertical whiskers indicate the minimum and maximum values within this interval. (g) The record of [MeHg] from the P2010 core. As in (c), the red lines are data from earlier shallow cores at depths corresponding to the P2010 samples.

are correlative. The largest of the [THg] spikes in the P2010 core has a value of 46.20 ng L^{-1}, which is a ~70-fold enrichment relative to the geometric mean [THg] in the core. This feature might represent fallout from the 1991 eruption of Hekla in Iceland (Gudmundsson et al., 1992). An episodic source of Hg deposition in Arctic snow originating from Iceland has long been suspected (Siegel et al., 1973), and the 1991 Hekla eruption produced a noticeable enrichment of trace metals, including Hg, in central Greenland snow (Gabrielli et al., 2008). The section of the P2010 firn core containing elevated [THg] is 1.63 m long, which is much thicker than the mean annual firn accumulation. If the elevated THg spikes were indeed the result of volcanic fallout, then the Hg deposited in the fallout may have been subsequently remobilized in firn by summer melt and percolation.

Apart from the section with anomalously high [THg] between 10 and 12 m, there are indications in the P2010 core that atmospheric Hg accumulation increased in recent decades (Fig. 6e), and the possible reasons for this are examined in Section 3.3. The variations in [MeHg] in the P2010 core (Fig. 6g) are small compared to [THg], and no systematic trends or patterns are discernible over the period 1970–2010, although the coarse sampling resolution may hide short-term variations. On average, [MeHg] accounts for 18 ± 14% of the [THg] in the common depth intervals over which both parameters were measured. This mean value is close to what was reported for Arctic glacier snowpacks in other studies (Larose et al., 2010; St-Louis et al., 2005; Zdanowicz et al., 2013).

3.3. Possible controls for the THg accumulation on Penny Ice Cap

The mean [THg] in the firn layers accumulated since 1990 in the P2010 core (0.90 ng L^{-1}; $N = 105$) is approximately twice the value in the older layers (0.47 ng L^{-1}; $N = 79$), and the difference is statistically significant (Wilcoxon rank sum test, $\alpha = 0.05$, $p \ll 0.01$). This comparison excludes the high values (>5 ng L^{-1}) found in the depth interval of 10–12 m. If the latter are included, the mean [THg] for the post-1990 period rises to 1.06 ng L^{-1}. The mass loading of accumulated firn (expressed as H_2O water equivalent per unit area) shows an essentially unvarying positive linear trend over the depth interval of the core, and any changes in the accumulation rate of THg (A_{THg}) over this interval must be governed by changes in [THg] (Fig. 7). In contrast, the mass loading of THg in the firn has been increasing non-linearly since the 1980s. A quadratic fit of the mass loading data produces an R^2 goodness-of-fit measurement of >0.99. A Monte-Carlo simulation performed with 50,000 random rearrangements of sample [THg] values and thicknesses shows that it is extremely unlikely for the observed non-linear trend to have arisen by chance alone. Our depth–age model for the P2010 core suggests that the increased A_{THg} began in the 1980s. The positive trend in [THg] from the 1980s to 2010 is statistically significant, even if a 10-fold reduction of freedom is assumed in the data series as a result of smearing by the post-depositional elution (Mann–Kendall test, $\alpha = 0.05$, $p \ll 0.01$). The presence of higher [THg] values in the shallow firn layers could explain why two short firn cores taken in 2007 near the P2010 site produced a mean A_{THg} of 0.33 µg m^{-2} a^{-1} (Zdanowicz et al., 2013), which is relatively elevated compared to the 40-year mean over the entire P2010 core.

These findings raise questions of whether the increasing trend in A_{THg} found in the P2010 core is observed at other Arctic sites or limited to Penny Ice Cap and what possible explanations might account for the trend. Presently, there are very few records available from the Arctic region to which the P2010 core can be directly compared. The firn record

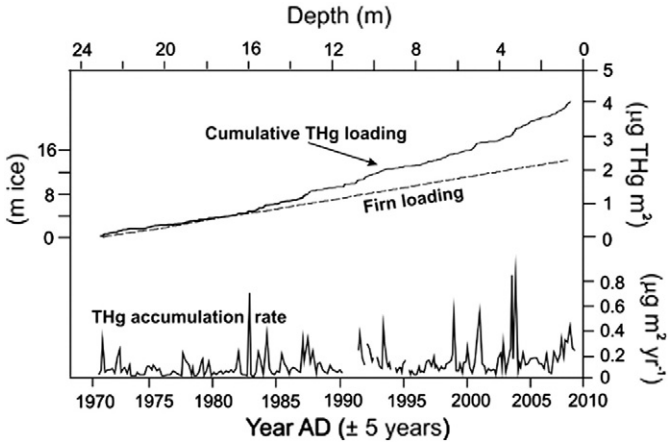

Fig. 7. Top: Trends in the cumulative mass loading of THg and firn with respect to ice-equivalent depth in the P2010 core. Bottom: Inferred interannual variations of the THg accumulation rate (A_{THg}) for the period 1970–2010 that were calculated assuming an unchanging mean firn accumulation of 0.40 m H_2O a^{-1}.

from Agassiz Ice Cap, Ellesmere Island, shows a higher mean [THg] in the post-1990 layers relative to earlier decades, but a parallel record from Mt. Oxford Icefield, which is ~200 km away, shows no sustained or monotonic increases over the same period (Zheng et al., 2014: Figs. 5c and 6f). Published records of THg in firn from Greenland are discontinuous and have been developed with various methods, which makes interpreting the long-term trends difficult. Brooks et al. (2011) reported [THg] values between 2.6 and 4.1 ng L^{-1} (arithmetic mean = 3.0 ng L^{-1}) in firn layers over the decade ~1998–2008 (Figs. 5d and 6f), and the values are noticeably higher than those previously found by Boutron et al. (1998) over the period 1949–1989 (≤2 ng L^{-1}; mean ~0.6 ng L^{-1}). These data could indicate a recent increase in Hg deposition in central Greenland, but this remains to be confirmed with a homogeneous continuous record.

Even with an unchanging atmospheric Hg burden, the deposition and accumulation in glacial firn may vary as a result of multiple environmental factors, including the availability of halogen radicals in the atmospheric boundary layer, which promote the conversion of Hg^0 to Hg^{2+} as reactive gas or particles (Steffen et al., 2008), the abundance of sea salt aerosols, which may enhance scavenging of Hg^{2+} and its deposition in snow (Malcolm et al., 2009), and the snow accumulation rate, which may limit post-depositional re-emission of Hg to the atmosphere (Durnford et al., 2012). The firn mass loading increases linearly over the length of the P2010 core, which suggests a relatively constant accumulation rate over the time interval represented by the core. Furthermore, an analysis of precipitation records from weather stations in the southern Baffin Island region (see Fig. 1 for location) did not reveal any large variations or meaningful trends over the period from 1970 to 2010.

The main source of marine aerosols (sea salt and other) on Penny Ice Cap is thought to be nearby Baffin Bay (Grumet et al., 2001). We examined time series of [Cl^-] and [nssSO_4^{2-}] in relation to [THg] in the P2010 core for possible evidence of a link between marine aerosol transport from this area and A_{THg} (Fig. 6b). Although some intervals in the core (e.g., the 1990s) show relatively elevated Cl^-, nssSO_4^{2-} and THg levels, no statistically meaningful correlation was found between these species, even when data were averaged over 1- to 3-m core lengths to account for different mobilities of major ions and Hg species during summer melt-induced elution in the firn. Our earlier pilot study also failed to reveal any significant correlations between [THg], [nssSO_4^{2-}] and [Cl^-] in the snow of the ice cap (Zdanowicz et al., 2013). Therefore, the observed increase in A_{THg} in the P2010 core cannot be accounted for by changes in firn accumulation and/or marine aerosol inputs, although we acknowledge that relationships between these variables could be obscured by the effects of post-depositional melt and percolation in the core. This does not rule out a possible link between THg accumulation on Penny Ice Cap and nearby sea surface conditions. The interval over which the increase in A_{THg} is observed in the P2010 core corresponds to a period (after ~1990) when the sea-ice cover and sea-ice concentration in particular began to experience a rapid (and ongoing) decline in Baffin Bay and Hudson Strait (Tivy et al., 2011). A reduced and more seasonally variable sea-ice cover in this area might allow a greater evasion of Hg^0 from seawater, such as in ice leads, while promoting the production of halogen radicals such as BrO from seasonal ice, which enhance the Hg deposition to snow (Moore et al., 2014). This might also impact the deposition on terrestrial snow and glacier firn if the marine boundary layer air masses are rapidly advected inland (Spolaor et al., 2013). The limited temporal resolution of the P2010 core does not currently allow this link to be fully investigated, but it deserves further scrutiny in future research.

Another possibility is that variations in A_{THg} in Penny Ice Cap for the period 1970–2010 are linked to changes in the frequency of airborne transport of Hg and/or marine aerosols from one or more specific geographic sector(s). For example, Sepp and Jaagus (2010) observed that the largest increase in the frequency of deep cyclones (carrying southerly air and moisture) entering the Arctic over the late 20th century occurred in the Baffin Bay — western Greenland region (between 48 and 80° W), which is on a cyclone track that delivers much of the precipitation to Penny Ice Cap. To investigate changes in air-mass provenance, we computed anomalies in the frequency of the 10-day air-mass back-trajectories arriving at the summit of Penny Ice Cap from 8 different geographic sectors for the period 1970–2010 (see Supporting information for detailed methods). The results were divided between the warm and wet (summer + autumn) months and cold and dry (winter + spring) months of the year. Meteorological stations (Fig. 1) from the southern Baffin Island region attest that over the 40-year period in consideration, an average of 67 ± 6% of the annual precipitation was delivered between June and November (incl.) and the remaining 33 ± 6% was delivered between December and May (incl.). The calculated mean frequencies of air mass sources divided by the sector of origin were approximately the same in all of the seasons (Table 2), with ~90% of all air masses originating from the Arctic Ocean (29 ± 1%), North America (24 ± 2%), North Atlantic Ocean (19 ± 3%), and CAA (18 ± 1%). These regions were not necessarily the source(s) of Hg transported in the air masses; however, our analysis provided an indication of the relative importance of airborne Hg transport vectors from different geographic quadrants to Penny Ice Cap.

The time series of air-mass transport frequency from the four dominant geographic sectors were compared to the THg, Cl^- and SO_4^{2-} accumulation trends in the P2010 core (Fig. 8). However, no obvious correlations could be established between these data for the period 1970–2010. For example, we could tentatively attribute part of the enhanced A_{THg} in the 1990s to the more frequent wintertime advection of airborne Hg (or marine aerosols) from the Arctic Ocean sector, but this inference was not applicable to the subsequent decade when the relative frequency of air mass transport from this sector actually declined as the A_{THg} continued to increase. Hence, the data did not indicate if the changing atmospheric transport patterns played any role in

Table 2
Relative frequency (%) of air mass provenance at Penny Ice Cap summit, based on daily air mass back-trajectory analysis.

	DJF	MAM	JJA	SON	MEAN
Arctic Ocean	30	29	31	28	29
North America	22	23	23	26	24
Atlantic Ocean	16	23	19	16	19
Can. Arctic Islands	17	19	19	17	18
Greenland	4	4	4	3	4
Pacific Ocean	3	2	1	4	3
Asia	3	2	2	3	2
Europe	2	1	0	1	1

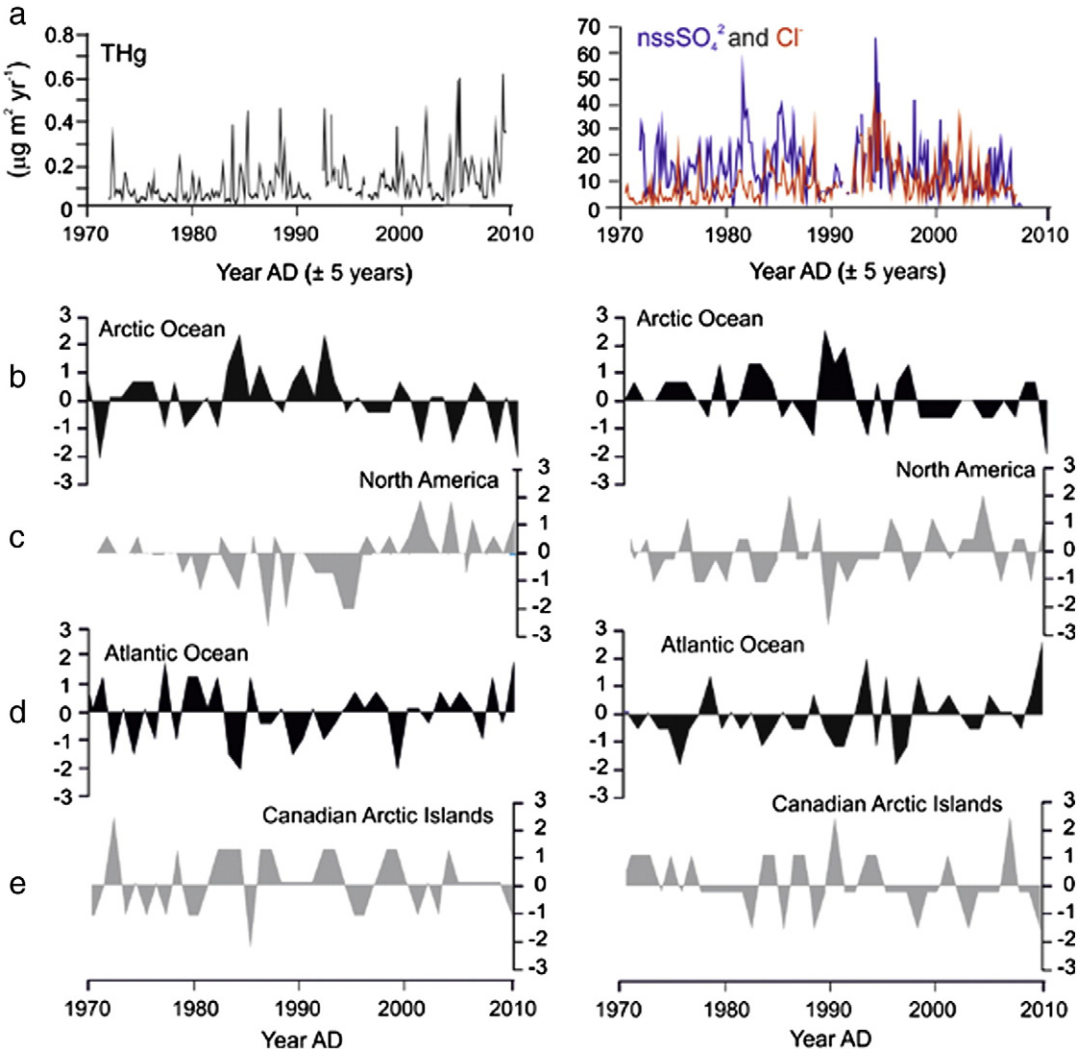

Fig. 8. (a) Variations in net atmospheric accumulation of THg (black), nssSO_4^{2-} (blue) and Cl^- (red) on Penny Ice Cap over the period 1970–2010 that were calculated from the P2010 firn core data. In (b) to (e), the relative frequencies are shown in the air mass advection to the summit of Penny Ice Cap summit from four different geographic regions based on the daily back-trajectory computations. Left: winter and spring (December to May). Right: summer and autumn (June to November). See Supporting information for a definition of the geographic domains.

modulating the decadal- or sub-decadal THg, Cl^- and/or SO_4^{2-} accumulation rates at Penny Ice Cap, which was possibly a result of the mixing of different air masses or shortness of the records.

4. Summary and conclusions

The key findings from our analysis of the P2010 firn record of SO_4^{2-}, THg and MeHg are summarized below.

(i) The extended record of nssSO_4^{2-} deposition obtained by combining the P95 and P2010 cores shows a comparable mean [nssSO_4^{2-}] in the firn layers from the 1960s to 1970s and from the most recent decade. This is inconsistent with various observations that indicate declining levels of SO_4^{2-} in the Arctic atmosphere over the past ~35–40 years. A possible explanation is that declining inputs of anthropogenic nssSO_4^{2-} on Penny Ice Cap are compensated by a greater influx of marine-derived nssSO_4^{2-} aerosols linked to the declining sea-ice cover conditions in the nearby Baffin Bay and Hudson Strait.

(ii) The record of THg accumulation in the P2010 core contains elevated spikes (up to 46 ng L^{-1}) in the firn layers dating from the early to mid-1990s. We tentatively attribute the largest of these spikes to fallout from the 1991 eruption of Hekla (Iceland), which also resulted in trace metal enhancements in the snow in central Greenland (Gabrielli et al., 2008).

(iii) Levels of MeHg deposited on Penny Ice Cap show little variation over the period from 1970 to 2010 and account for 18% of the THg in the firn.

(iv) We have found evidence in the P2010 core that THg accumulation on Penny Ice Cap has increased since the 1980s relative to the earlier part of the 20th century. This increase cannot be easily explained by changes in factors such as snow accumulation (preservation of Hg in snow), marine aerosol inputs (scavenging effect), or air mass trajectories (Hg transport from specific geographic sectors); however, a link may exist with the declining sea-ice cover in nearby marine areas over the same period, which might have promoted the production of halogen radicals and enhanced Hg deposition in the snow. Because of the rapid changes that are currently occurring to the Canadian Arctic sea-ice environment, this possible link should be a focus for future investigations.

(v) The estimated increase in THg accumulation on Penny Ice Cap between the pre-industrial (late Holocene) and modern industrial era (post-1850) is estimated at between 4- and 16-fold, which is consistent with a range of estimates obtained from Arctic lake sediment cores.

The new THg record from Penny Ice Cap is the first record developed from the Baffin Island region of the eastern Canadian Arctic and one of few such records presently available in the Arctic; it provides a new perspective on the trends and magnitude of Hg accumulation in glaciated environments and complements other archives such as lake sediments. We hope that this record (and others like it) helps to bridge the knowledge gap between direct observation of gaseous Hg in the Arctic atmosphere and actual net deposition and accumulation in various terrestrial media.

Acknowledgments

Field sampling was conducted with the assistance of A. Smetny-Sowa and the Parks Canada staff. We thank the hamlet of Pangnirtung, Nunavut, for local support. Charter air transport was provided by the Polar Continental Shelf Project. J. Sekerka performed the ionic analyses at GSC, whereas B. Wang, A. Smetny-Sowa, K. Fuller and B. Main assisted with the cold room procedures. This project was supported by Natural Resources Canada (NRCan), the Northern Contaminant Program and the International Polar Year (Aboriginal Affairs and Northern Development Canada).

Appendix A. Supplementary material

Data and Supporting information related to this article can be found online at http://dx.doi.org/10.1016/j.scitotenv.2014.04.092

References

Bindler R, Renberg I, Appleby PG, Anderson NJ, Rose NL. Mercury accumulation rates and spatial patterns in lake sediments from west Greenland: a coast to ice margin transect. Environ Sci Technol 2001;35(9):1736–41.
Boutron CF, Candelone J-P, Hong S. Greenland snow and ice cores: unique archives of large-scale pollution of the troposphere of the Northern Hemisphere by lead and other heavy metals. Sci Total Environ 1995;160–161:233–41.
Boutron CF, Vandal GM, Fitzgerald WF, Ferrari CP. A forty year record of mercury in central Greenland snow. Geophys Res Lett 1998;25:3315–8.
Brooks S, Moore C, Lew D, Lefer B, Huey G, Tanner D. Temperature and sunlight controls of mercury oxidation and deposition atop the Greenland ice sheet. Atmos Chem Phys 2011;11:8295–306.
Buck CF, Mayewski PA, Spencer MJ, Whitlow S, Twickler MS, Barrett D. Determination of major ions in snow and ice cores by ion chromatography. J Chromatogr 1992;594:225–8.
Cai Y, Jaffe R, Alli A, Jones RD. Determination of organomercury compounds in aqueous samples by capillary gas chromatography–atomic fluorescence spectrometry following solid-phase extraction. Anal Chim Acta 1996;334:251–9.
Cole AS, Steffen A, Aspmo FK, Berg T, Pilote M, Poissant L, et al. Ten-year trends of atmospheric mercury in the high Arctic compared to Canadian sub-Arctic and mid-latitude sites. Atmos Chem Phys 2013;13:1535–45.
Cooke CA, Wolfe AP, Michelutti N, Balcom PH, Briner JP. A Holocene perspective on algal mercury scavenging to sediments of an Arctic lake. Environ Sci Technol 2012;46:7135–41.
Dansgaard W, Johnsen SJ. A flow model and a time scale for the ice core from Camp Century, Greenland. J Glaciol 1969;8:215–23.
Douglas A, Loseto LL, Macdonald RW, Outridge P, Dommergue A, Poulain AF, et al. The fate of mercury in Arctic terrestrial and aquatic ecosystems, a review. Environ Chem 2012;9(4):321–55.
Draxler RR, Hess GD. An overview of the HYSPLIT 4 modelling system for trajectories, dispersion, and deposition. Aust Meteorol Mag 1998;47:295–308.
Drevnick PE, Muir DG, Lamborg CH, Horgan MJ, Canfield DE, Boyle JF, et al. Increased accumulation of sulfur in lake sediments of the High Arctic. Environ Sci Technol 2010;44:8415–21.
Durnford DA, Dastoor AP, Steen AO, Berg T, Ryzhkov A, Figueras-Nieto D, et al. How relevant is the deposition of mercury onto snowpacks? — part 1: a statistical study on the impact of environmental factors. Atmos Chem Phys 2012;12:9221–49.
Environmental Protection Agency US. US-EPA Method 1631, Revision E: mercury in water by oxidation, purge and trap, and cold vapor atomic fluorescence spectrometry. EPA-821-R-02-019. Washington: US-EPA; 2002 [38 pp.].
Faïn X, Ferrari CP, Dommergue A, Albert M, Battle M, Arnaud L, et al. Mercury in the snow and firn at Summit Station, Central Greenland, and implications for the study of past atmospheric mercury levels. Atmos Chem Phys 2008;8:3441–57.
Fischer H, Wagenbach D, Kipfstuhl J. Sulfate and nitrate concentrations on the Greenland ice sheet. 1 — large-scale geographical deposition changes. J Geophys Res 1998;103(D17):21,927–34.
Fisher D, Reeh N, Clausen HB. Stratigraphic noise in time series derived from ice cores. Ann Glaciol 1985;7:76–83.
Fisher DA, Koerner RM, Bourgeois J, Zielinski G, Wake C, Hammer C, et al. Penny Ice Cap cores, Baffin Island, Canada, and the Wisconsinan Foxe Dome connection: two states of Hudson Bay ice cover. Science 1998;279:692–5.
Gabrielli P, Barbante C, Plane JMC, Boutron CF, Jaffrezo JL, Mather TA, et al. Siderophile metal fallout from the 1991 winter eruption of Hekla (Iceland) and during the global atmospheric perturbation of Pinatubo. Chem Geol 2008;255:78–86.
Gong SL, Zhao TL, Sharma S, Toom-Sauntry D, Lavoué D, Zhang XB, et al. Identification of trends and interannual variability of sulfate and black carbon in the Canadian High Arctic: 1981–2007. J Geophys Res 2010;115:D07305. http://dx.doi.org/10.1029/2009JD012943.
Goodsite M, Outridge PM, Christensen JH, Dastoor A, Muir D, Travnikov O, et al. How well do environmental archives of atmospheric mercury deposition in the Arctic reproduce rates and trends depicted by atmospheric models and measurements? Sci Total Environ 2013;452–453:196–207.
Goto-Azuma K, Koerner RM. Ice core studies of anthropogenic sulfate and nitrate trends in the Arctic. J Geophys Res 2001;206(D5):4959–69.
Goto-Azuma K, Nakawo M, Shimizu M, Azuma N, Nakayama M, Yokoyama K. Temporal changes in chemical stratigraphy of snow cover. Ann Glaciol 1993;18:86–91.
Goto-Azuma K, Koerner RM, Fisher DA. An ice-core record over the last two centuries from Penny Ice Cap, Baffin Island, Canada. Ann Glaciol 2002;35:29–35.
Grumet NS, Wake CP, Zielinski GA, Fisher DA, Koerner RM, Jacobs JJ. Preservation of glaciochemical time-series in snow and ice from Penny Ice Cap, Baffin Island. Geophys Res Lett 1998;25:357–60.
Grumet NS, Wake CP, Mayewski PA, Zielinski GA, Whitlow SI, Koerner RM, et al. Variability of sea-ice extent in Baffin Bay over the last millennium. Clim Change 2001;49:129–45.
Gudmundsson A, Oskarsson N, Gronvold K, Saemundsson K, Sigurdsson O, Stefansson R, et al. The 1991 eruption of Hekla, Iceland. Bull Volcanol 1992;54:238–46.
Harder S, Warren SG, Charlson RG. Sulfate in air and snow at the South Pole: implications for transport and deposition at sites with low snow accumulation. J Geophys Res 2000;105(D18):22,825–32.
Hirdman D, Burkhart JF, Sodemann H, Eckhardt S, Jefferson A, Quinn PK, et al. Long-term trends of black carbon and sulphate aerosol in the Arctic: changes in atmospheric transport and source region emissions. Atmos Chem Phys 2010;10:9351–68.
Holdsworth GH. Glaciological reconnaissance of an ice core drilling site, Penny Ice Cap, Baffin Island. J Glaciol 1984;30:3–15.
Kinnard C, Zdanowicz C, Fisher D, Alt B, McCourt S. Climatic analysis of sea ice variability in the Canadian Arctic from operational charts, 1980–2004. Ann Glaciol 2006;44:391–402.
Koerner RM, Fisher D. Acid snow in the Canadian High Arctic. Nature 1982;295:137–40.
Larose C, Dommergue A, DeAngelis M, Cossa D, Averty B, Marusczak N, et al. Springtime changes in snow chemistry lead to new insights into mercury methylation in the Arctic. Geochim Cosmochim Acta 2010;74:6263–75.
Law KS, Stohl A. Arctic air pollution: origins and impacts. Science 2007;315:1537–40.
Li S-M, Barrie LA. Biogenic sulfur aerosol in the Arctic troposphere: 1. Contributions to total sulfate. J Geophys Res 1993;98(Dl1):20,613–22.
Malcolm EG, Ford AC, Redding TA, Richardson MC, Strain BM, Tetzner SW. Experimental investigation of the scavenging of gaseous mercury by sea salt aerosol. J Atmos Chem 2009;63:221–34.
McConnell JR, Edwards R. Coal burning leaves toxic heavy metal legacy in the Arctic. Proc Natl Acad Sci U S A 2008;105:12,140–4.
McConnell JR, Edwards R, Kok GL, Flanner MG, Zender CS, Saltzman ES, et al. 20th-century industrial black carbon emissions altered Arctic climate forcing. Science 2007;317:1381–4.
Mekis É, Vincent LA. An overview of the second generation adjusted daily precipitation dataset for trend analysis in Canada. Atmos Ocean 2011;2:163–77.
Moore CW, Obrist D, Steffen A, Staebler RM, Douglas TA, Richter A, et al. Convective forcing of mercury and ozone in the Arctic boundary layer induced by leads in sea ice. Nature 2014. http://dx.doi.org/10.1038/nature12924.
Muir DCG, Wang X, Yang F, Nguyen N, Jackson TA, Evans MS, et al. Spatial trends and historical deposition of mercury in eastern and northern Canada inferred from lake sediment cores. Environ Sci Technol 2009;43:4802–9.
Pasteris DR, McConnell JR, Edwards R. High-resolution, continuous method for measurement of acidity in ice cores. Environ Res Technol 2012;46:1659–66.
Quinn PK, Bates TS, Baum E, Doubleday N, Fiore AM, Flanner M, et al. Short-lived pollutants in the Arctic: their climate impact and possible mitigation strategies. Atmos Chem Phys 2008;8:1723–35.
Quinn PK, Bates TS, Schulz K, Shaw GE. Decadal trends in aerosol chemical composition at Barrow, Alaska: 1976–2008. Atmos Chem Phys 2009;9:8883–8.
Rempillo O, Séguin AM, Norman A-L, Scarratt M, Michaud S, Chang R, et al. Dimethyl sulfide air-sea fluxes and biogenic sulfur as a source of new aerosols in the Arctic fall. J Geophys Res 2011;116(D00S04). http://dx.doi.org/10.1029/2011JD016336.
Sepp M, Jaagus J. Changes in the activity and tracks of Arctic cyclones. Clim Change 2010;105:577–95.
Siegel BZ, Siegel SM, Thorarinsson F. Icelandic geothermal activity and the mercury of the Greenland ice cap. Science 1973;241:526.
Smith SJ, van Aardenne J, Klimont Z, Andres RJ, Volke A, Delgado Arias SD. Anthropogenic sulfur dioxide emissions: 1850–2005. Atmos Chem Phys 2011;11:1101–16.
Spolaor A, Gabrieli J, Martma T, Kohler J, Björkman MB, Isaksson E, et al. Sea ice dynamics influence halogen deposition to Svalbard. Cryosphere 2013;7:1645–58.
Steffen A, Douglas T, Amyot M, Ariya PA, Aspmo K, Berg T, et al. A synthesis of atmospheric mercury depletion event chemistry linking atmosphere, snow and water. Atmos Chem Phys 2008;8:1445–82.
St-Louis V, Sharp M, Steffen A, May A, Barker J, Kirk J, et al. Some sources and sinks of monomethyl and inorganic mercury on Ellesmere Island in the Canadian High Arctic. Environ Sci Technol 2005;39:2686–701.

Streets DG, Devane MK, Lu Z, Bond TC, Sunderland EM, Jacob DJ. All-time releases of mercury to the atmosphere from human activities. Environ Sci Technol 2011;45:10,485–91.

Thorarinsson S, Sigvalddason GE. The Hekla eruption of 1970. Bull Volcanol 1972;36:269–88.

Tivy A, Howell SEL, Alt B, McCourt S, Chagnon R, Crocker G, et al. Trends and variability in summer sea ice cover in the Canadian Arctic based on the Canadian Ice Service Digital Archive, 1960–2008 and 1968–2008. J Geophys Res 2011;116:C03007. http://dx.doi.org/10.1029/2009JC005855.

Toyota K, Dastoor A, Rhyskov A. Air–snowpack exchange of bromine, ozone and mercury in the springtime Arctic simulated by the 1-D model PHANTAS — part 2: mercury and its speciation. Atmos Chem Phys Discuss 2013;13:22,151–220.

United Nations Environment Programme. Report of the intergovernmental negotiating committee to prepare a global legally binding instrument on mercury on the work of its fifth session, Geneva; 2013 [13–18 January 2013, 69 pp.].

Vincent LA, Wang XL, Milewska EJ, Wan H, Yang F, Swail V. A second generation of homogenized Canadian monthly surface air temperature for climate trend analysis. J Geophys Res 2012;117:D18110. http://dx.doi.org/10.1029/2012JD017859.

Wolfe AP, Cooke CA, Hobbs WO. Are current rates of atmospheric nitrogen deposition influencing lakes in the eastern Canadian Arctic? Arct Antarct Alp Res 2006;38(3):465–76.

Zdanowicz C, Smetny-Sowa A, Fisher D, Schaffer N, Copland L, Eley J. Summer melt rates on Penny Ice Cap, Baffin Island: past and recent trends, and implications for regional climate. J Geophys Res 2012;117:F02006. http://dx.doi.org/10.1029/2011JF002248.

Zdanowicz C, Krümmel E, Lean D, Poulain A, Yumvihoze E, Chen J, et al. Accumulation, storage and release of atmospheric mercury in a glaciated Arctic catchment, Baffin Island, Canada. Geochim Cosmochim Acta 2013;107:316–35.

Zheng J, Kudo A, Fisher D, Blake E, Gerasimoff M. Solid electrical conductivity (ECM) from four Agassiz ice cores, Ellesmere Island NWT, Canada: high-resolution signal and noise over the last millennium and low resolution over the Holocene. The Holocene 1998;8:413–21.

Zheng J, Fisher D, Blake E, Hall G, Vaive J, Zdanowicz C, et al. An ultra-clean firn core from the Devon Island Ice Cap, Nunavut, Canada, retrieved using a titanium drill specially designed for trace element studies; 2006.

Zheng J, Pelchat P, Vaive J, Bass D, Ke F. Total mercury in snow samples from Canadian High Arctic ice caps and glaciers: a practical procedure for total Hg quantification at low pg g^{-1} levels. Sci Total Environ 2014;468–469:487–94.